Supporting Information

Luminescent iridium(III) complexes as COX-2-specific imaging agents in cancer cells

Chenfu Liu,[‡a] Chao Yang,[‡b] Lihua Lu,[‡ac] Wanhe Wang,[‡a] Weihong Tan,[*de] Chung-Hang Leung,[*b] and Dik-Lung Ma[*a]

[a] Department of Chemistry, Hong Kong Baptist University, Kowloon Tong, Hong Kong, China. E-mail: edmondma@hkbu.edu.hk
[b] State Key Laboratory of Quality Research in Chinese Medicine, Institute of Chinese Medical Sciences, University of Macau, Macao, China. E-mail: duncanleung@umac.mo
[c] College of Chemistry and Pharmaceutical Sciences, Qingdao Agricultural University, Qingdao 266109, China
[d] Department of Chemistry and Department of Physiology and Functional Genomics, Center for Research at the Bio/Nano Interface, Shands Cancer Center, UF Genetics Institute, McKnight Brain Institute, University of Florida, Gainesville, USA. E-mail: tan@chem.ufl.edu
[e] Molecular Sciences and Biomedicine Laboratory, State Key Laboratory for Chemo/Biosensing and Chemometrics, College of Chemistry and Chemical Engineering and College of Biology, Collaborative Innovation Center for Molecular Engineering and Theranostics, Hunan University, Changsha, China.

General experimental. Mass spectrometry was performed at the Mass Spectroscopy Unit at the Department of Chemistry, Hong Kong Baptist University, Hong Kong (China). Deuterated solvents for NMR purposes were obtained from Armar and used as received. ^{1}H and ^{13}C NMR were recorded on a Bruker Avance 400 spectrometer operating at 400 MHz (^{1}H) and 100 MHz (^{13}C). ^{1}H and ^{13}C chemical shifts were referenced internally to solvent shift (acetone-d_6: ^{1}H δ 2.05, ^{13}C δ 29.8; DMSO-d_6: ^{1}H δ 2.50, ^{13}C δ 39.52; $CDCl_3$: ^{1}H δ 7.26, ^{13}C δ 77.16). Chemical shifts (δ) are quoted in ppm, the downfield direction being defined as positive. Uncertainties in chemical shifts are typically ±0.01 ppm for ^{1}H and ±0.05 for ^{13}C. Coupling constants are typically ±0.1 Hz for ^{1}H-^{1}H and ±0.5 Hz for ^{1}H-^{13}C couplings. The following abbreviations are used for convenience in reporting the multiplicity of NMR resonances: s, singlet; d, doublet; t, triplet; q, quartet; m, multiplet; br, broad. All NMR data were acquired and processed using standard Bruker software (Topspin).

Syntheses. 2-(1-(4-chlorobenzyl)-5-methoxy-2-methyl-1*H*-indol-3-yl) acetic acid (**4**). Compound **4** was synthesized according to a literature report.[1]

Yield: 52%. ^{1}H NMR (400 MHz, $CDCl_3$) δ 2.29 (s, 3H), 3.73 (s, 2H), 3.84 (s, 3H), 5.22 (s, 2H), 6.77 (dd, 1H, *J* = 2.4 Hz, 8.8 Hz), 6.86 (d, 2H, *J* = 8.4 Hz), 7.02 (d, 1H, *J* = 2.4 Hz), 7.04 (d, 1H, *J* = 8.8 Hz), 7.22 (d, 2H, *J* = 8.4 Hz);^{13}C NMR (100 MHz, $CDCl_3$) δ 10.4, 30.4, 46.2, 55.9, 100.4, 103.8, 109.8, 111.2, 127.3, 128.1, 129.0, 131.4, 133.1, 135.0, 136.3, 154.4, 177.1; The spectroscopic data is consistent with the previous report.[1]

2-(1-(4-chlorobenzyl)-5-methoxy-2-methyl-1*H*-indol-3-yl)-*N*-(1,10-phenanthrolin-5-yl) acetamide (**4a**).

To a stirred solution of compound **4** (770 mg, 2.24 mmol) in dichloromethane (10 mL) at room temperature were added oxalyl chloride (0.21 mL, 2.48 mmol) and anhydrous *N*,*N*-dimethylformamide (18 μL, 0.234 mmol). The mixture was stirred for 2 h at room temperature. 1, 10-phenanthrolin-5-amine (436.8 mg, 2.24 mmol) was then added, and the mixture was stirred overnight at room temperature. The reaction mixture was diluted with water and dichloromethane. The organic layer was washed with saturated $NaHCO_3$ solution and then brine. The organic layer was dried over anhydrous Na_2SO_4, filtered, and concentrated *in vacuo*.[2] The pure product **4a** was obtained by column chromatography (MeOH /CH_2Cl_2 = 1: 50 as eluent).

Yield: 55%.^{1}H NMR (400 MHz, DMSO) δ 2.41 (s, 3H), 3.77 (s, 3H), 3.95 (s, 2H), 5.39 (s, 2H), 6.71 (dd, 1H, *J* = 2.4 Hz, 8.8 Hz), 7.01 (d, 2H, *J* = 8.0 Hz), 7.26-7.36 (m, 4H), 7.72 (dd, 1H, *J* = 4.4 Hz, 8.0 Hz), 7.76 (dd, 1H, *J* = 4.4 Hz, 8.4 Hz), 8.15 (s, 1H), 8.42 (dd, 1H, *J* = 1.6 Hz, 8.0 Hz), 8.57 (d, 1H, *J* = 8.4 Hz), 9.02 (dd, 1H, *J* = 1.6 Hz, 4.0 Hz), 9.12 (dd, 1H, *J* = 1.6 Hz, 4.4 Hz), 10.28 (s, 1H); ^{13}C NMR (100 MHz, DMSO) δ 10.4, 32.3, 45.3, 55.5, 100.7, 105.5, 110.0, 110.1, 120.3, 122.7, 123.6, 124.7, 128.1, 128.2, 128.6, 131.1, 131.4, 131.6, 131.8, 135.2, 135.8, 137.7, 143.8, 145.8, 149.3, 149.9, 153.6, 170.8; HRMS cacld for $C_{31}H_{26}ClN_4O_2$ $[M+H]^+$: 521.1749, found 521.1739.

2-(1-(4-chlorobenzoyl)-5-methoxy-2-methyl-1*H*-indol-3-yl)-*N*-(1,10-phenanthrolin-5-yl) acetamide (**5a**).

The procedure followed was the same as that detailed above, using compound **5** instead of compound **4**.

Yield: 42%.^{1}H NMR (400 MHz, $CDCl_3$) δ 2.52 (s, 3H), 3.79 (s, 3H), 3.99 (s, 2H), 6.76 (dd, 1H, *J* = 2.0 Hz, 8.8 Hz), 6.89 (d, 1H, *J* = 8.8 Hz), 7.08 (d, 1H, *J* = 2.0 Hz), 7.41 (dd, 1H, *J* = 4.0 Hz, 8.4 Hz), 7.48 (d, 2H, *J* = 8.4 Hz), 7.58 (dd, 1H, *J* = 4.4 Hz, 8.0 Hz), 7.67-7.71 (m, 3H), 8.15-8.24 (m, 3H), 9.07 (t, 2H, *J* = 2.0 Hz). ^{13}C NMR (100 MHz, $CDCl_3$) δ 13.4, 33.1, 55.8, 100.9, 112.2, 112.5, 115.4, 119.6, 122.8, 123.5, 123.9, 128.2, 129.3, 129.4, 129.9, 130.1, 131.0, 131.2, 133.2, 136.1, 136.9, 139.8, 149.7, 150.0, 156.5, 168.3, 169.2; HRMS cacld for $C_{31}H_{24}ClN_4O_3$ $[M+H]^+$: 535.1531, found 535.1534.

Complexes **1** and **2** were synthesized according to the literature report.[3] A solution of ligand **4a** or **5a** (0.031 mmol), dichloro-bridged $[Ir(ppy)_2Cl]_2$ (15 mg, 0.014 mmol) in dichloromethane (3 mL) and methanol (3 mL) was stirred at room temperature

overnight. After the reaction completed, an excess of solid NH_4PF_6 was added and stirred for another 0.5 h at room temperature. The mixture was filtered, and the solvent was removed under reduced pressure. The residue was purified by silica gel column chromatography (eluent, methanol/dichloromethane, 1:50, *v*/*v*) to yield the product as a yellow powder (precipitated by ethyl ether).

Complex **1**. Yield: 53%. ^{1}H NMR (400 MHz, acetone) δ 2.49 (s, 3H), 3.78 (s, 3H), 4.11 (s, 2H), 5.46 (s, 2H), 6.43 (d, 2H, *J* = 7.6 Hz), 6.77 (d, 1H, *J* = 8.8 Hz), 6.94-6.99 (m, 4H), 7.06-7.09 (m, 4H), 7.27-7.30 (m, 3H), 7.66 (t, 2H, *J* = 5.6 Hz), 7.87-8.00 (m, 7H), 8.22 (d, 2H, *J* = 8.0 Hz), 8.32 (d, 1H, *J* = 4.8 Hz), 8.42 (d, 1H, *J* = 4.8 Hz), 8.68-8.73 (m, 2H), 8.81 (d, 1H, *J* = 8.4 Hz), 9.64 (s, 1H). ^{13}C NMR (100 MHz, acetone) δ 10.9, 30.1, 46.7, 56.2, 101.7, 111.6, 115.6, 120.8, 123.6, 124.5, 125.9, 127.3, 128.1, 129.0, 129.6, 131.3, 132.4, 132.7, 132.8, 139.6, 150.4, 151.1, 152.2, 168.7, 169.0; HRMS calcd for $C_{53}H_{41}ClIrN_6O_2$ $[M\text{-}PF_6]^+$: 1021.2599, found 1021.2625.

Complex **2**. Yield: 65%. ^{1}H NMR (400 MHz, acetone) δ 2.46 (s, 3H), 3.80 (s, 3H), 4.14 (s, 2H), 6.44 (dd, 2H, *J* = 4.0 Hz, 7.6 Hz), 6.73-6.75 (m, 1H), 6.94-7.01 (m, 5H), 7.07 (t, 2H, *J* = 7.6 Hz), 7.28 (d, 1H, *J* = 1.6 Hz), 7.62-7.67 (m, 4H), 7.76 (d, 2H, *J* = 8.0 Hz), 7.87-7.93 (m, 4H), 7.98-8.05 (m, 2H), 8.22 (d, 2H, *J* = 8.4 Hz), 8.34 (d, 1H, *J* = 4.8 Hz), 8.45 (d, 1H, *J* = 4.8 Hz), 8.68 (d, 1H, *J* = 6.4 Hz), 8.78-8.82 (m, 1H), 8.92 (d, 1H, *J* = 8.4 Hz), 9.85 (s, 1H); ^{13}C NMR (100 MHz, acetone) δ 13.8, 33.1, 56.1, 102.7, 112.3, 115.9, 117.7, 120.8, 123.6, 124.4, 125.9, 127.4, 128.1, 130.0, 131.3, 131.3, 132.0, 132.2, 132.7, 132.7, 134.9, 135.2, 135.5, 137.3, 139.2, 139.4, 139.5, 145.2, 145.2, 150.4, 151.0, 151.3, 152.3, 157.2, 168.7, 168.7, 169.0, 170.7, 170.8; HRMS calcd for $C_{53}H_{39}ClIrN_6O_3[M\text{-}PF_6]^+$:1035.2391, found 1035.2371.

Complex **3**. Reported.[4]

Photophysical measurement. Emission spectra, lifetime measurements and luminescence quantum yields were determined according to a reference.[5]

Effect of pH, ions, amino acids and other macromolecules. 0.5 mM of complex stock solution was prepared by dissolving complex **1** in acetonitrile. For effect of pH, the complex was then added into PBS buffer with indicated pH to a final concentration of 1 μM. For ions, different ions were added to PBS buffer with pH = 7.2 containing complex **1** (1 μM) in a cuvette, which final concentration of the ions is 1 mM. For amino acids and other macromolecules, the analyte was added to PBS buffer with pH = 7.2 containing complex **1** (1 μM) in a cuvette, which final concentration of the analyte is 10 μM. Luminescence emission spectra were recorded on a PTI QM-4

spectrofluorometer (Photo Technology International, Birmingham, NJ) at 25 °C, with the slits for both excitation and emission set at 2.5 nm.

Materials and cell lines. All chemicals were bought from Sigma-Aldrich and were used as received. XTT assay kit was purchased from Cayman Chemical (Ann Arbor, MI, USA). Fetal bovine serum (FBS) and Dulbecco's Modified Eagle's Medium (DMEM) were available from Gibco BRL (Gaithersburg, MD, USA). Human serum albumin (HSA) and bovine serum albumin (BSA) were also purchased from Sigma-Aldrich (St. Louis, MO). Other reagents and chemicals were obtained from commercial sources.

Cell cultures. All cell lines were purchased from the American Type Culture Collection (Manassas, VA, USA). Cells were cultured in DMEM supplemented with 10% fetal bovine serum (FBS) and in 5% CO_2 in a 37 °C incubator.

Immunoblotting. Cells (1×10^6 cells/well) were treated with indicated concentrations of curcumin for 12 h. Cells were washed twice by pre-cold PBS. Protein samples were harvested by adding cell lysis buffer. After electrophoresis of protein samples (30 μg of total protein) on SDS-PAGE gels, the samples were transferred to a PVDF membrane and incubated at room temperature with blocking solution for 1 h. The membrane was treated with primary antibodies and incubated overnight at 4 °C. After incubation with secondary antibodies (Santa Cruz Biotechnology), protein bands were visualized using ECL Western Blotting Detection Reagent (GE Healthcare).

XTT cell viability assay. Cells were seeded at the density of 5,000 cells per well in 96-well plates and incubated for 12 h. Complex **1** or complex **2** dissolved in DMSO was added to cells at final concentrations ranging from 1 nM to 100 μM for 72 h. Fifty μL of the prepared XTT mixture were added into each well and mixed gently for another 4 h. Before starting the test, the plate was shaken one min at room temperature in the dark. The cytotoxicity of complex **1** and **2** was shown as the percentage of absorbance in a SpectraMax M5 microplate reader at a wavelength of 450 nm.

Cell imaging. Cell lines were cultured 2 days in DMEM medium with 10% FBS and penicillin/streptomycin in a 5% CO_2 incubator at 37°C. Before imaging, cells were seeded into a glass-bottomed dish (35 mm dish with 20 mm well). After 24 h, the cells were incubated with complex **1** or complex **2** for indicated time and then washed with

phosphate-buffered saline three times. The fluorescence imaging of complexes **1** and **2** in cells was carried out by a Leica TCS SP8 confocal laser scanning microscope system. The excitation wavelength was 405 nm.

Table S1 Photophysical properties of iridium(III) complex **1**.

Complex	Quantum yield	λ_{em} / nm	Lifetime / μs	UV/Vis absorption λ_{abs} / nm (ε / $dm^3\,mol^{-1}\,cm^{-1}$)
1	0.058	575	4.56	230 (5.70×10^4), 256 (5.27×10^4), 346 (1.46×10^4), 393 (1.03×10^4)
2	0.088	580	4.284	230 (7.45×10^4), 255 (8.2×10^4), 336 (2.46×10^4), 388 (1.0×10^4)

(a)

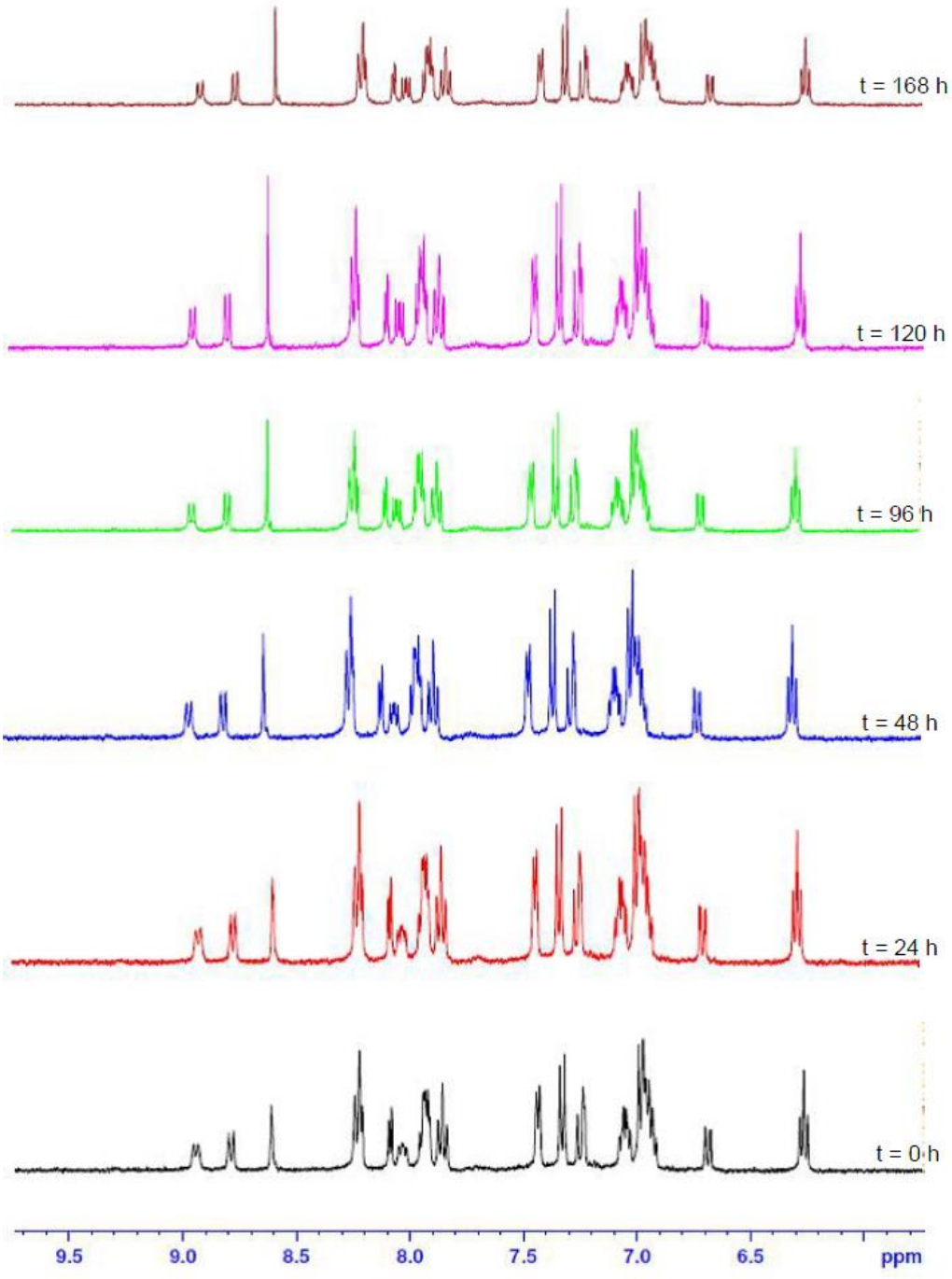

(b)

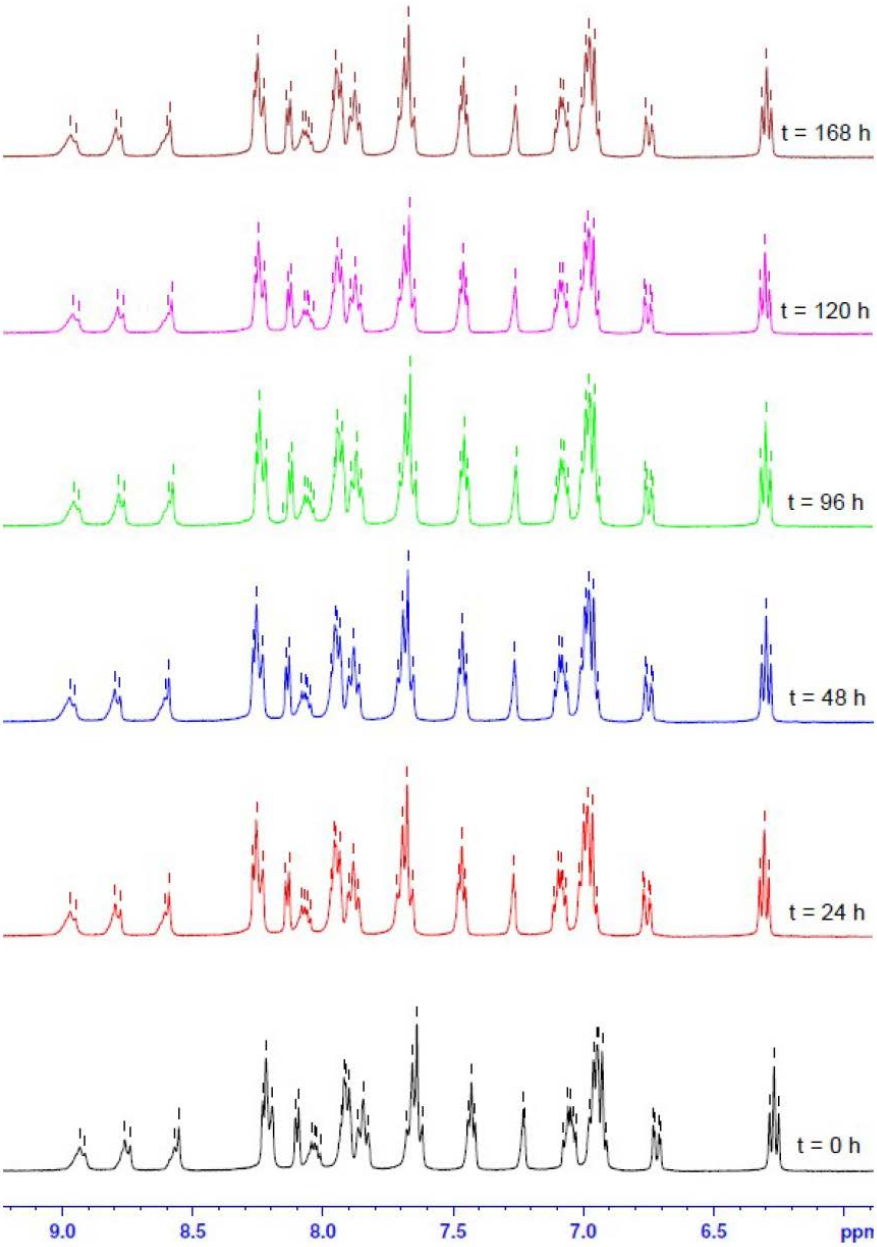

Fig. S1. Aromatic region of the ^{1}H NMR spectra of (a) complex **1** and (b) complex **2** at a concentration of 5 mM in 90% DMSO-d_6/10% D_2O at t = 0 h and after incubation for 24, 48, 96, 120 and 168 h at 298 K.

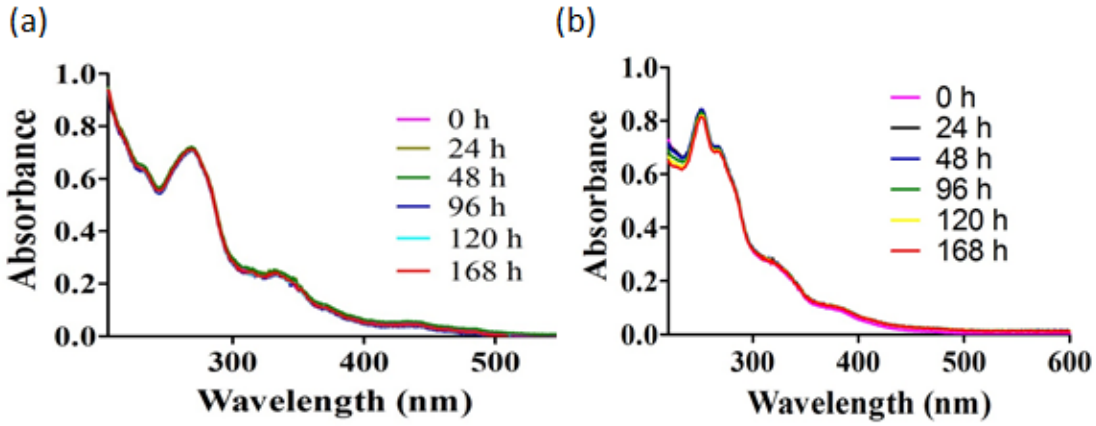

Fig. S2. UV/Vis absorption of (a) complex **1** and (b) complex **2** at a concentration of 1 μM in 80% acetonitrile/20% Tris-HCl buffer at t = 0 h and after incubation for 24, 48, 96, 120 and 168 h at 298 K. (Tris-HCl buffer with a concentration of 20 mM, containing 20 mM NaCl, pH = 7.5).

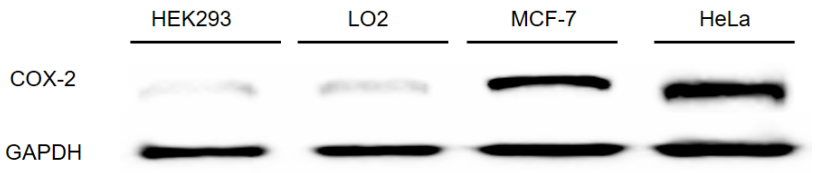

Fig. S3. Immunoblotting analysis of COX-2 levels in human embryonic kidney 293 cells, human liver LO2 cells, human breast adenocarcinoma MCF-7 cells and human cervical cancer HeLa cells.

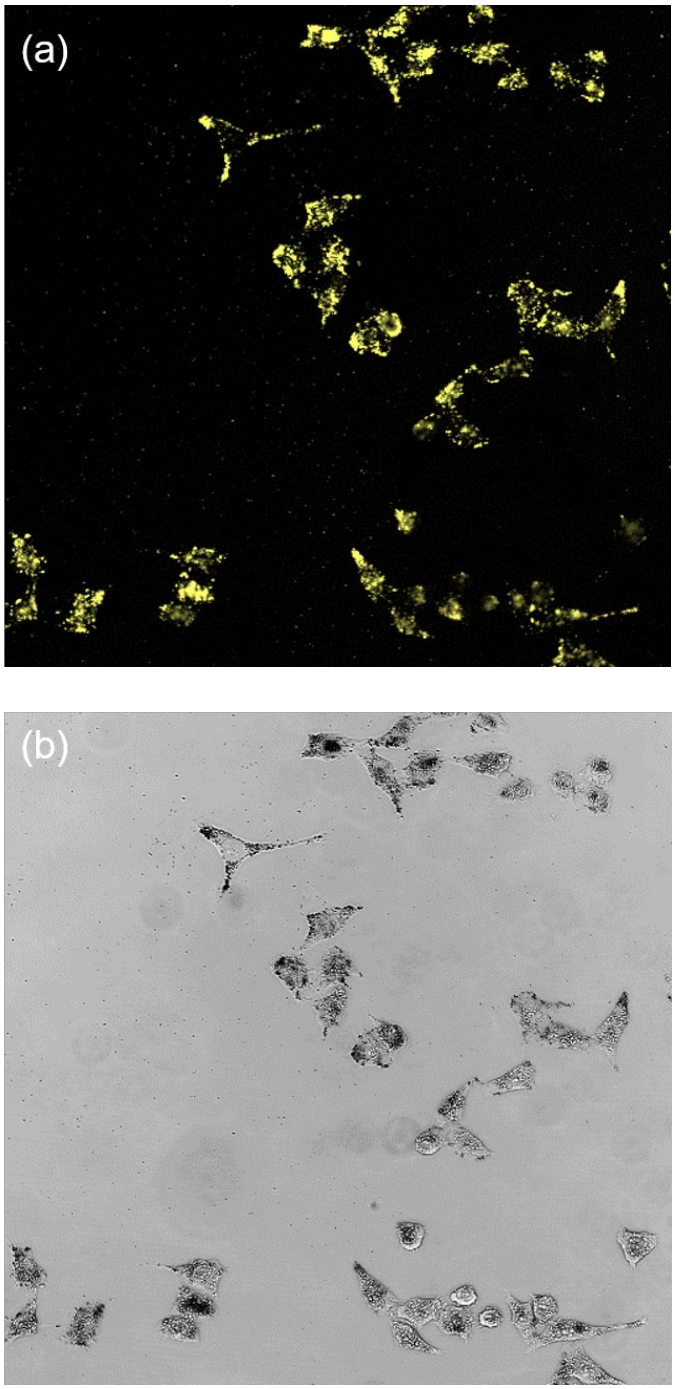

Fig. S4. Living HeLa cells stained with complex **2** (1 μM). (a) fluorescence imaging (b) bright filed imaging. Excitation wavelength = 405 nm.

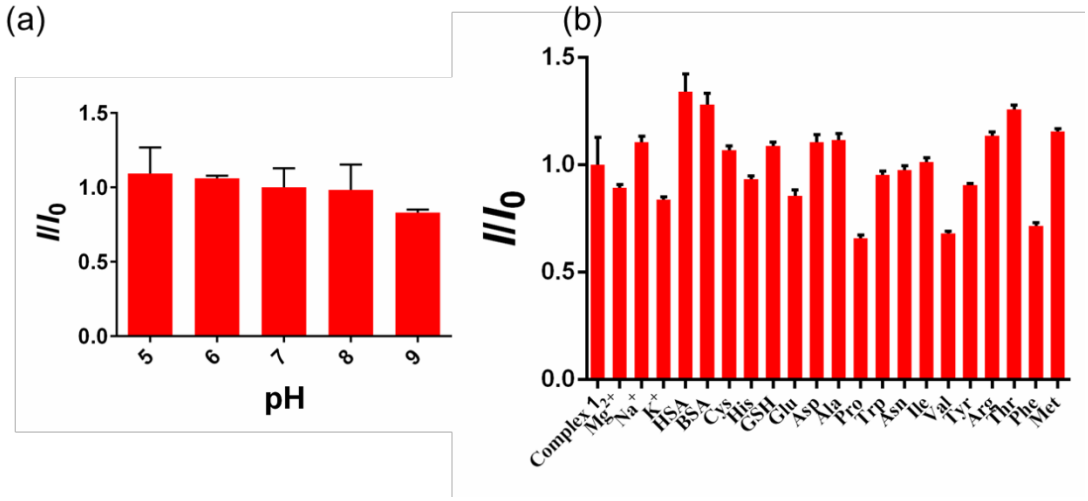

Fig. S5 (a) Luminescence intensity of complex **1** (1 μM) at different pH values. (b) Luminescence intensity of complex **1** (1 μM) in the presence of various ions, amino acids, BSA and HSA. "*I* "is the luminescence intensity of complex **1** in the presence of the analytes, while "I_0" is the luminescence intensity of complex **1** alone.

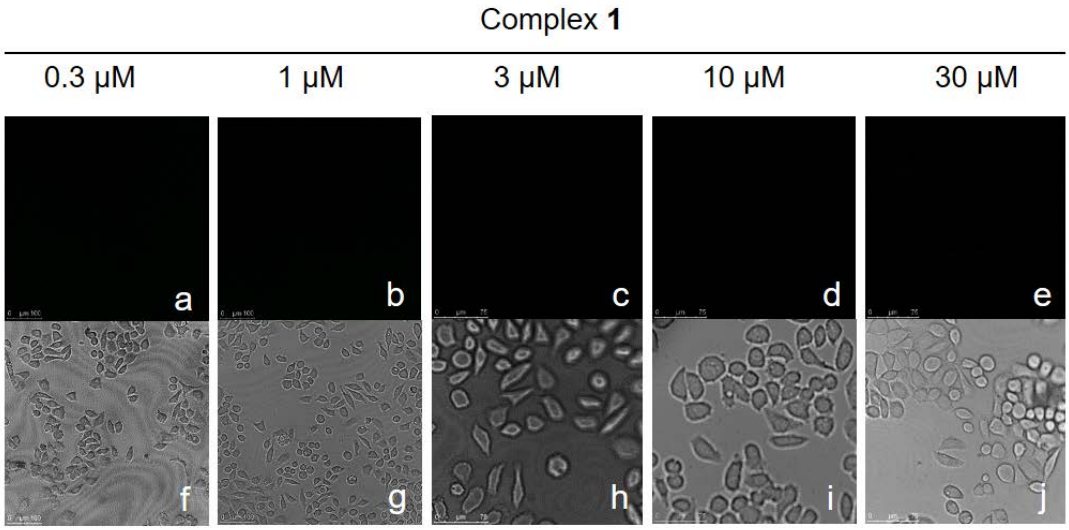

Fig. S6. Normal cell line (LO2) stained by different concentration of complex **1** (0.3, 1, 3, 10 and 30 μM). The upper row is fluorescence imaging, and the lower row is bright filed imaging. Excitation wavelength = 405 nm.

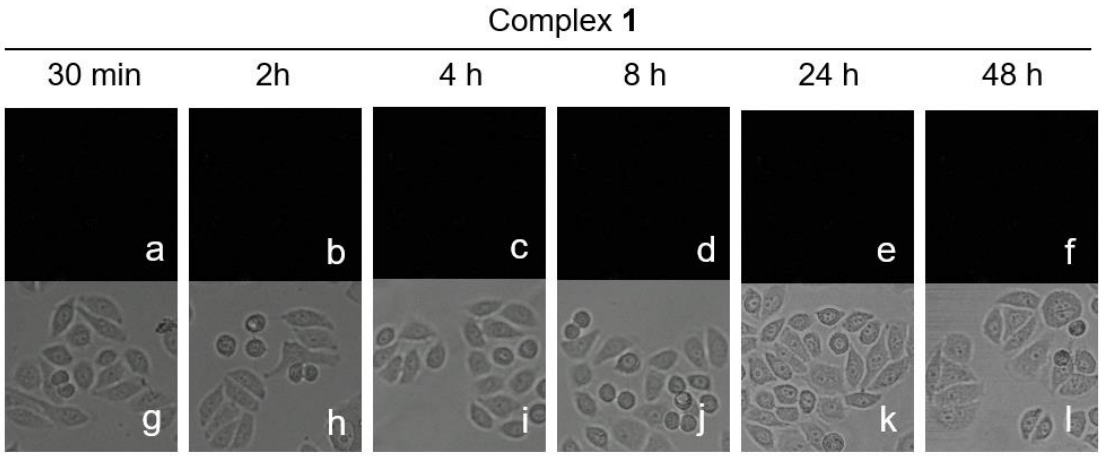

Fig. S7. Normal cell line (LO2) stained by complex **1** (1 μM) at different incubation time (0.5, 1, 2, 4, 8, 24 h). The upper row (a, b, c, d, e and f) is fluorescence imaging, and the lower row (g, h, i, j, k and l) is bright filed imaging. Excitation wavelength = 405 nm.

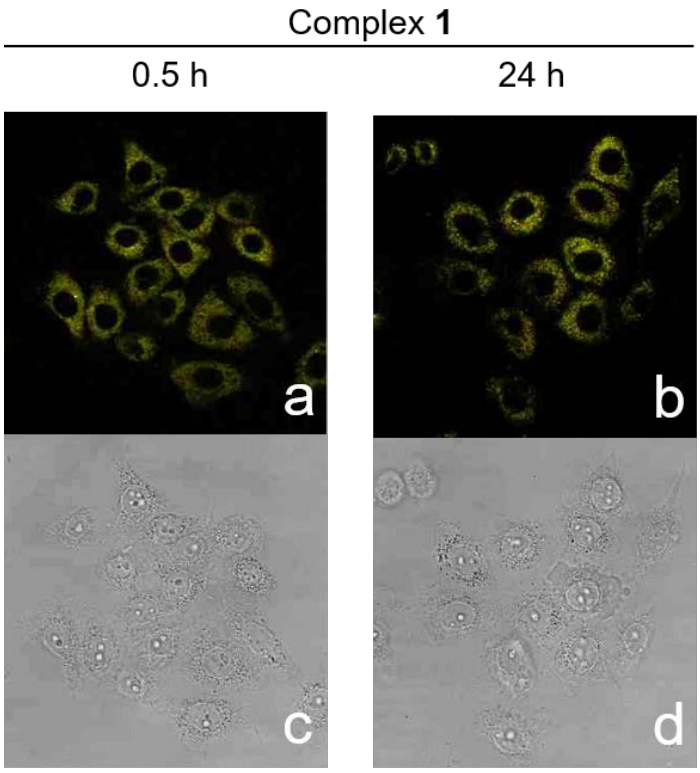

Fig. S8. Living HeLa cells stained with complex **1** (1 μM). (a, b) fluorescence images and (c, d) bright filed images. Excitation wavelength = 405 nm.

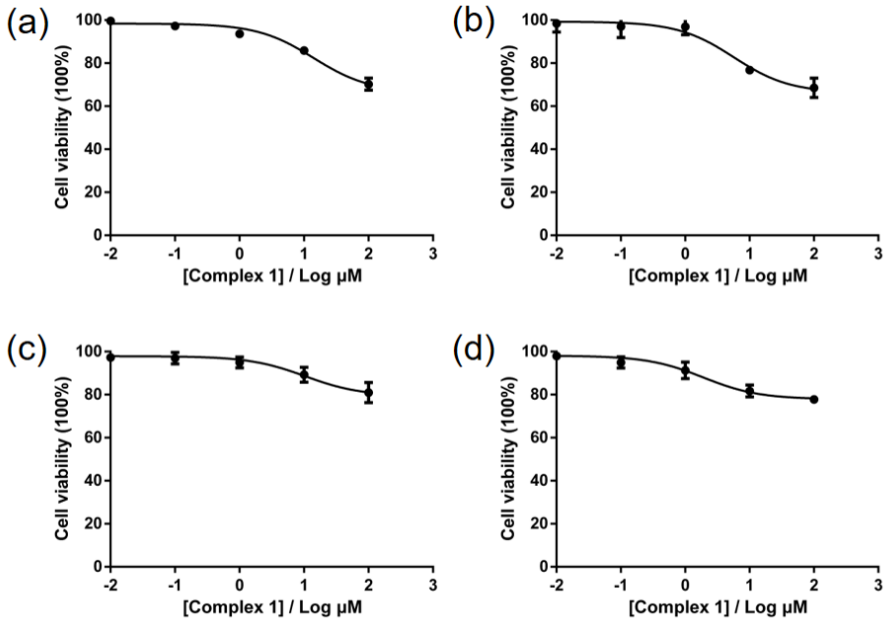

Fig. S9. Cytotoxic effect of complex **1** on (a) human embryonic kidney 293 cells, (b) human liver LO2 cells, (c) human cervical cancer HeLa cells, and (d) human breast adenocarcinoma MCF-7 cells, as determined by XTT assay. Cells were exposed to the indicated concentrations of complex **1** for 72 h. Complex **1** inhibited the growth of the HEK293 cells, LO2 cells, MCF-7 cells and HeLa cells with an IC_{50} value > 100 μM. Error bars represent the standard deviations of the results from three independent experiments.

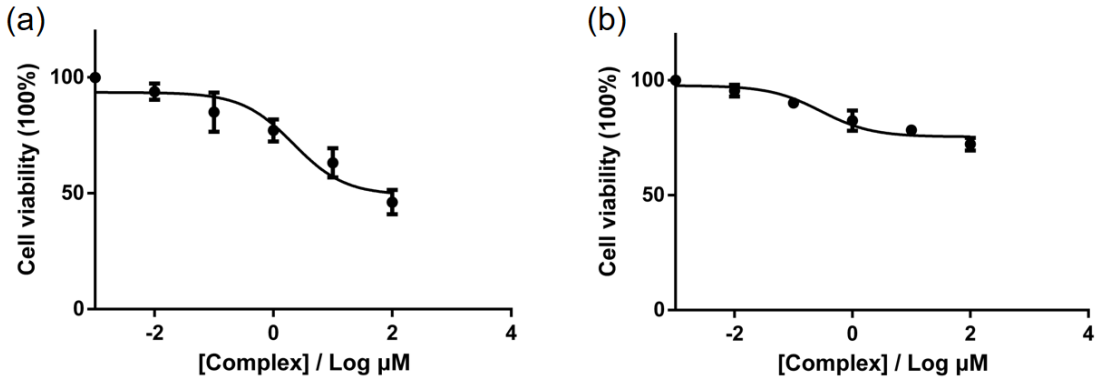

Fig. S10. Cytotoxic effect of complex **2** on (a) human liver LO2 cells and (b) human cervical cancer HeLa cells. The data were determined by XTT assay. Cells were exposed to the indicated concentrations of complex **2** for 72 h. Complex **2** inhibited the growth of LO2 cells with IC_{50} values of 55.6 μM and HeLa cells with IC_{50} values > 100 μM, respectively. Error bars represent the standard deviations of the results from three independent experiments.

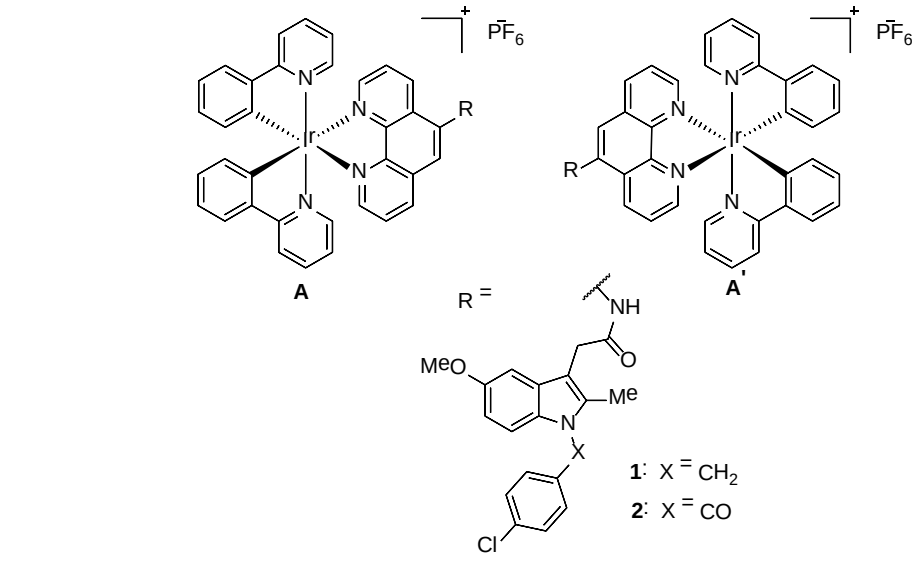

Fig. S11. Two stereoisomers of Ir(III) complexes **1** and **2**.

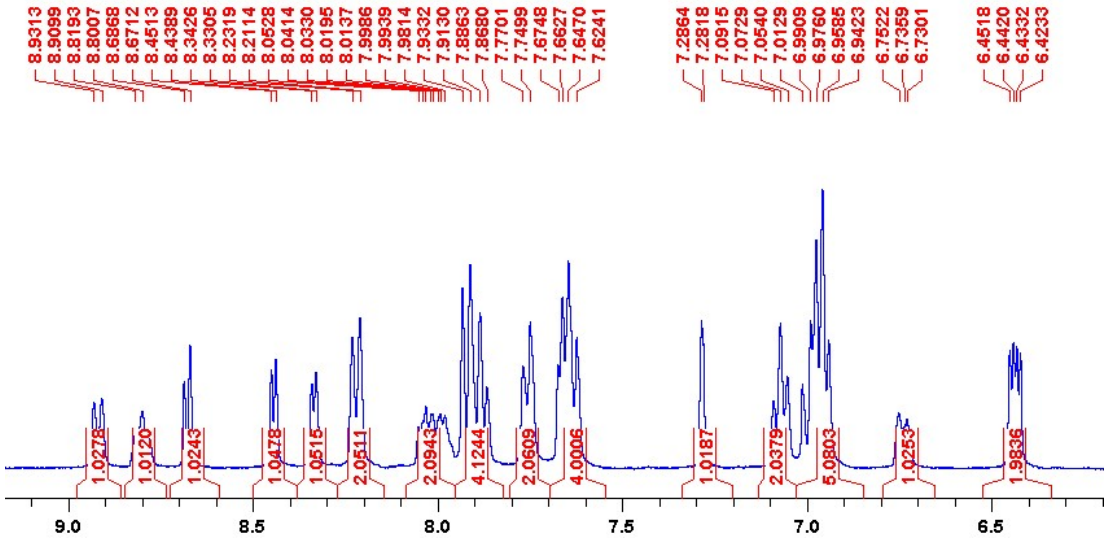

Fig. S12. Partial ^{1}H NMR spectrum of complex **2**.

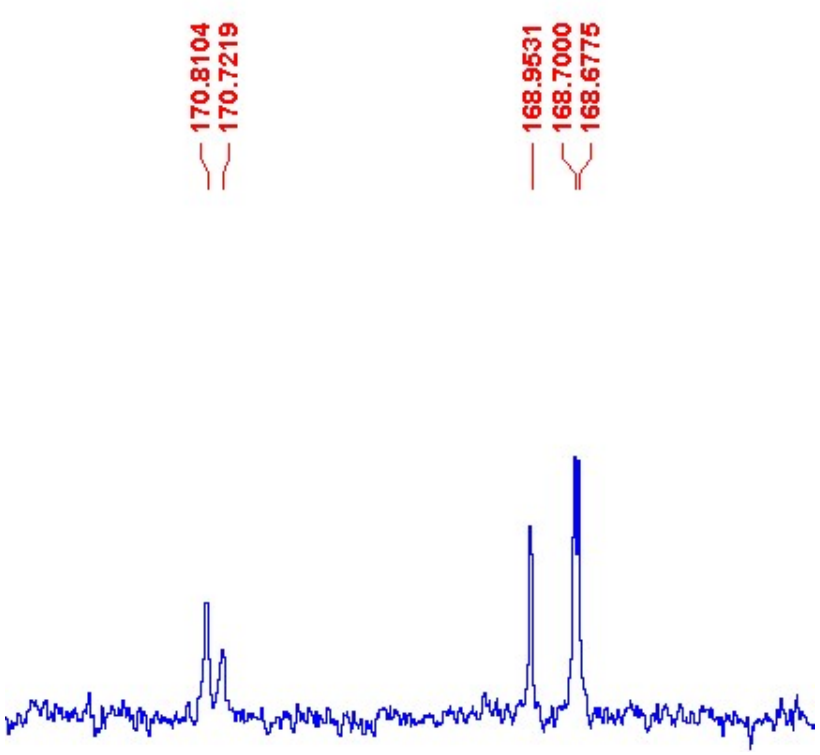

Fig. S13. Partial ^{13}C NMR spectrum of complex **2**

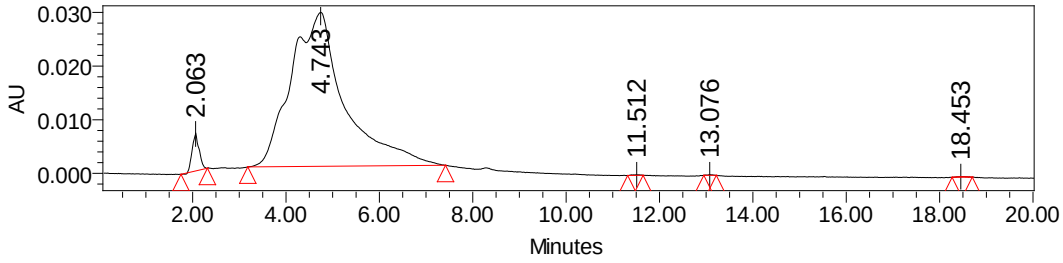

	Name	Retention Time	Area	% Area	Height	Int Type	Peak Type
1		2.063	72932	3.07	6891	bb	Unknown
2		4.743	2299022	96.77	28712	bb	Unknown
3		11.512	1387	0.06	106	bb	Unknown
4		13.076	918	0.04	117	bb	Unknown
5		18.453	1498	0.06	103	bb	Unknown

Fig. S14. HPLC chromatogram of complex **1** using 30% H_2O and 70% MeOH as eluent.

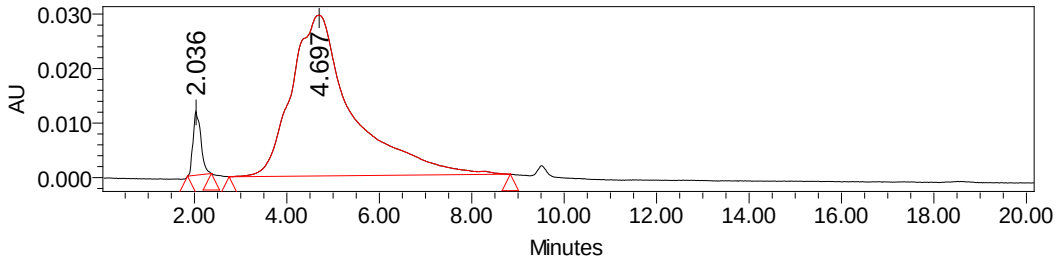

	Name	Retention Time	Area	% Area	Height	Int Type	Peak Type
1		2.036	136822	4.82	11549	bb	Unknown
2		4.697	2704463	95.18	29501	bb	Unknown

Fig. S15. HPLC chromatogram of complex **2** using 30% H_2O and 70% MeOH as eluent.

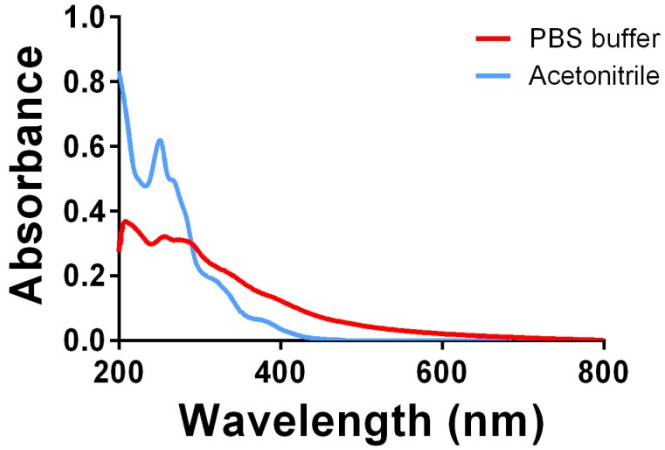

Fig. S16. UV/Vis spectra of complex **1** (1 μM) in acetonitrile and PBS buffer (pH = 7.4).

References:

1 A. R. Maguire, S. J. Plunkett, S. Papot, M. Clynes, R. O'Connor and S. Touhey, *Bioorganic & medicinal chemistry*, 2001, **9**, 745.

2 D. Boyer, J. N. Bauman, D. P. Walker, B. Kapinos, K. Karki and A. S. Kalgutkar, *Drug Metabolism and Disposition*, 2009, **37**, 999.

3 L. Lu, D. S.-H. Chan, D. W. Kwong, H.-Z. He, C.-H. Leung and D.-L. Ma, *Chemical Science*, 2014, **5**, 4561.

4 C. Dragonetti, L. Falciola, P. Mussini, S. Righetto, D. Roberto, R. Ugo, A. Valore, F. De Angelis, S. Fantacci and A. Sgamellotti, *Inorganic chemistry*, 2007, **46**, 8533.

5 M. Wang, Z. Mao, T.-S. Kang, C.-Y. Wong, J.-L. Mergny, C.-H. Leung and D.-L. Ma, *Chemical Science*, 2016, **7**, 2516.